Journal of Translational Medicine

RESEARCH

Open Access

m6A-modified circXPO1 accelerates colorectal cancer progression via interaction with FMRP to promote WWC2 mRNA decay

Xiaowen Zhu[1,2] and Pengxia Zhang[1*]

Abstract

Background Recent evidence has demonstrated the vital roles of circular RNAs (circRNAs) in the progression of colorectal cancer (CRC); however, their functions and mechanisms in CRC need to be further explored. This study aimed to uncover the biological function of circXPO1 in CRC progression.

Methods CircXPO1 was identified by Sanger sequencing, RNase R, and actinomycin D treatment assays. Colony formation, scratch, transwell assays, and mouse xenograft models were adopted to evaluate CRC cell growth and metastasis in vitro and in vivo. Subcellular expression of circXPO1 was detected by FISH and nuclear-cytoplasmic separation assays. Molecular mechanisms were investigated by MeRIP, RIP, and RNA pull-down assays. Target molecular expression was detected by RT-qPCR, Western blotting and immunohistochemical staining.

Results circXPO1 was up-regulated in CRC tissues and cells, which indicated a poor prognosis of CRC patients. circXPO1 deficiency delayed the growth, EMT, and metastasis of CRC cells. Mechanistical experiments indicated that down-regulation of ALKBH5 enhanced IGF2BP2-mediated m6A modification of circXPO1 to increase circXPO1 expression. Furthermore, circXPO1 interacted with FMRP to reduce the mRNA stability of WWC2, which consequently resulted in Hippo-YAP pathway activation. Rescue experiments suggested that WWC2 overexpression abrogated circXPO1-mediated malignant capacities of CRC cells. The in vivo growth and liver metastasis of CRC cells were restrained by circXPO1 depletion or WWC2 overexpression.

Conclusions m6A-modified circXPO1 by ALKBH5/IGF2BP2 axis destabilized WWC2 via interaction with FMRP to activate Hippo-YAP pathway, thereby facilitating CRC growth and metastasis. Targeting circXPO1 might be a potential therapeutic strategy for CRC.

Keywords Colorectal cancer, circXPO1, m6A, WWC2, Hippo-YAP pathway

*Correspondence:
Pengxia Zhang
pengxiaz@163.com
[1]Key laboratory of Microecology-immune Regulatory Network and Related Diseases, School of Basic Medicine, Jiamusi University, No. 258 Xuefu Road, Xiangyang District, Jiamusi 154000, Heilongjiang Province, P. R. China
[2]General surgery, The first Affiliated Hospital of Jiamusi University, Jiamusi 154000, Heilongjiang Province, P. R. China

Introduction

Colorectal cancer (CRC) remains a prevalent gastrointestinal tract tumor, which ranks the second leading cause of death worldwide [1]. Metastasis, the primary cause of high mortality, greatly affects the prognosis of CRC patients [2]. Although great improvements have been made in diagnosis, surgical resection, chemoradiotherapy, and immunotherapy, the 5-year survival rate is still poor, especially for CRC patients with metastasis [3, 4]. Therefore, it is crucial to clarify the complicated pathogenesis of CRC to identify new therapeutic targets for CRC.

Circular RNAs (circRNAs) are a novel type of noncoding RNAs, characterized by covalently closed ring structure [5]. Unlike linear RNAs, circRNAs are resistant to degradation caused by RNA exonuclease due to the circular structure [6]. It has been recognized that dysregulation of circRNAs takes part in the tumorigenesis and development of various malignancies, including CRC [7]. For instance, circNOLC1 contributed to liver metastasis of CRC cells by sponging miR-212-5p or regulation of oxidative pentose phosphate pathway via interaction with AZGP1 [8]. High expression of circRNA_102051 was reported to facilitate the growth, invasion, and stemness of CRC cells via modulation of the miR-203a/BPTF axis [9]. circXPO1, a new identified circRNA, has been proved to promote the progression of multiple malignancies. For instance, circXPO1 was reported to drive the growth of multiple myeloma via regulation of the miR-495-3p/DDIT4 axis [10]. Another study documented that circXPO1 contributed to the malignant phenotypes of glioblastomas cells via targeting miR-7-5p [11]. Chen et al., reported that circXPO1 favored the progression of prostate cancer by sponging miR-23a [12]. Nevertheless, the role of circXPO1 in CRC remains obscure, which needs to be further explored.

N6-methyladenosine (m6A) is one of prevalent modifications in circRNAs. m6A modification exerts key roles in transcription, translation, localization, and stability of RNAs, and m6A can be dynamically regulated by methyltransferases, demethylases, and methylation reading proteins [13]. AlkB homolog 5, RNA demethylase (ALKBH5) is an important demethylase that can remove m6A modification from RNAs, thereby playing diverse biological functions [14]. In CRC, ALKBH5 was found to be lowly expressed, and ALKBH5 overexpression could delay CRC development via inhibiting m6A modification of PHF20 [15]. Insulin-like growth factor 2 mRNA-binding proteins (IGF2BP) are newly identified methylation reading proteins, including IGF2BP1, IGF2BP2, and IGF2BP3 [16]. Convincing evidence has demonstrated that IGF2BP1/2/3 mediate tumor bio-behavioral changes and regulate the progression of various tumors including CRC through m6A modification [17]. As predicted by bioinformatics analysis, circXPO1 possessed several m6A modification sites, and IGF2BP1/2/3 possessed potential binding sites on circXPO1. In addition, our preliminary experiment showed that ALKBH5 overexpression remarkably reduced circXPO1 expression in CRC cells, while other m6A modification-related enzymes (including METTL3, METTL14, and FTO) did not affect circXPO1 expression. Thus, we speculated that ALKBH5 might inhibit IGF2BP1/2/3-mediated m6A modification of circXPO1, and consequently reduced circXPO1 stability in CRC cells.

Hippo-YAP pathway is involved in the regulation of occurrence, metastasis, and chemoresistance of multiple cancers [18]. Mounting evidence has proved the promotive role of the Hippo-YAP pathway in the tumorigenesis of CRC [19]. WW and C2 domain containing 2 (WWC2) belongs to the WWC protein family, which has been demonstrated to restrain YAP transcription to negatively regulate Hippo-YAP signaling pathway, thereby repressing invasion and growth of cancer cells [20, 21]. A previous study found that WWC2 was down-regulated in CRC, and enhancement of WWC2 expression mediated by LINC00460 knockdown effectively repressed metastasis of CRC cells [22]. circRNAs have been identified to interact with RNA-binding proteins (RBPs) to regulate mRNA stability [23]. Notably, Cirinteractome database predicted that RBP fragile X mental retardation protein (FMRP) could interact with circXPO1. Besides, a direct interaction between FMRP and WWC2 was predicted by RPISeq database. Therefore, we predicted that m6A-modified circXPO1 might bind to FMRP to affect WWC2 mRNA stability during CRC progression.

In this work, we for the first time discovered the biological function of circXPO1 in CRC. The results indicated that down-regulation of ALKBH5 facilitated circXPO1 expression via promoting IGF2BP2-mediated m6A modification, and circXPO1 subsequently bound to FMRP to promote WWC2 mRNA decay, thus facilitating CRC cell growth and metastasis via activation of Hippo-YAP pathway. These findings uncover the oncogenic role of circXPO1 in CRC and suggest circXPO1 as an effective therapeutic target for CRC.

Materials and methods

Clinical sample collection

Fifty-six paired CRC tissues and adjacent peritumoral tissues were collected from CRC patients at School of Basic Medicine, Jiamusi University. All the CRC patients did not receive radiotherapy or chemotherapy before surgical resection. All tissue samples were immediately treated with liquid nitrogen and then stored at -80˚C. Informed consents were collected from all patients. This study was approved by the Ethics Committee of School of Basic Medicine, Jiamusi University.

Cell culture

Intestinal epithelial cell line FHC, and CRC cell lines (LoVo, SW480, SW620, HCT116, HCT-8) were obtained from American Type Culture Collection (VA, USA). The cells were cultured with RPMI 1640 (Thermo Fisher, MA, USA), or DMEM (Thermo Fisher) containing 10% FBS (Gibco, New York, USA) at 37 °C with 5% CO_2.

Cell transfection

Short hairpin RNA targeting circXPO1 (shcircXPO1, sequences: GAACCAGTGCGAAGTAATCTA), negative control shRNA (shNC, sequences: TTCTCCGAACGT GTCACGT), and positive control shRNA (shGAPDH, sequences: GCTCATTTCCTGGTATGACAA) were purchased from GenePharma (Shanghai, China). The full-length sequences of METTL3, METTL14, ALKBH5, FTO, IGF2BP2, FMRP, circXPO1, or WWC2 gene were subcloned into pcDNA3.1 vector to establish overexpression plasmids. CRC cells (4×10^5) were transiently transfected with shRNAs (500 ng/μL) or pcDNA3.1 plasmids (4 μg) using Lipofectamine 2000 (Thermo Fisher) for 48 h. The stably transfected cells were selected by treatment with 2 μg/mL puromycin for 4 weeks.

Circular structure confirmation

The circular structure of circXPO1was identified by RNase R treatment, actinomycin D assay, and sanger sequencing according to previously described methodology [24, 25]. For RNase R treatment, the total RNAs were isolated from CRC cells and then treated with RNase R (2 U/μg RNA, cat. no. 14606ES, Yeasen, Shanghai, China) for 30 min at 37 °C. Then, the levels of circXPO1 and linear XPO1 mRNA were measured by RT-qPCR. For actinomycin D assay, CRC cells were treated with 5 μg/mL actinomycin D (MCE, cat. no. HY-17559, NJ, USA) for 4 h, 8 h, 12 h, and 24 h. Subsequently, total RNAs were extracted from CRC cells and the expression of circXPO1 and linear XPO1 mRNA was assessed by RT-qPCR. For Sanger sequencing, circXPO1 was amplified using divergent primers and subcloned into T vector. Then, its head-to-tail splicing was determined by Sanger sequencing (Tsingke Biotechnology, Beijing, China).

RNA fluorescence in situ hybridization (FISH)

FAM-labeled circXPO1 probe (sequences: GCTGGCAT AGATTACTTCGCACTGGTTCCTTG) was purchased from GenePharma. FISH assay was conducted using the RNA FISH Kit (GenePharma). Briefly, CRC cells were planted into 6-well plates at a confluence of 30-50% were fixed with 4% formaldehyde, permeabilized by 0.5% Triton X-100 for 15 min and blocked by 1× blocking buffer. Subsequently, the CRC cells were incubated with circXPO1 probe at 37 °C for 16 h. After nuclear staining with DAPI, the cells were observed and photographed using a laser confocal microscopy (Olympus, Tokyo, Japan).

Nuclear and cytoplasmic separation

The nuclear and cytoplasmic fractions of CRC cells were separated using the Nuclear and Cytoplasmic Protein Extraction Kit (cat. no. P0027, Beyotime, Haimen, China). Then, RNAs were isolated from the nuclear and cytoplasmic fractions. circXPO1 expression was evaluated by RT-qPCR. GAPDH and U6 were used as cytoplasmic and nuclear control, respectively.

Colony formation assay

CRC cells with various treatments were planted into 6-well plates (700 cells per well). The cells were cultured at 37˚C under 5% CO_2 for 14 days. During this period, the culture medium was changed every 2–3 days. The colonies consisting of >50 cells were fixed with 4% paraformaldehyde for 20 min, stained with 0.1% crystal violet for 20 min at room temperature, photographed and quantified.

Scratch assay

CRC cells were seeded into 6-well plates (5×10^5 cells per well). After reaching 100% confluence, a straight scratch was made in CRC cells using a 200 μL pipette tip. The cells were imaged at 0 h and 24 h after incubation in serum-free medium at 37˚C under 5% CO_2. The wound healing rate was calculated as follow: (wound width$^{0\ h}$ – wound width$^{24\ h}$)/wound width $^{0\ h}\times100\%$.

Transwell assay

The invasion of CRC cells was evaluated using the Transwell chambers (8-μm pore size, Corning, MI, USA) pre-coated with matrigel (37˚C for 30 min). In brief, the lower chambers were added with 600 μL of complete culture medium containing 10% FBS. CRC cells (5×10^4) suspended in 200 μL of serum-free medium were seeded into the upper chambers. After incubation for 24 h, the non-invaded cells were scrubbed, and the invaded cells were fixed with 4% paraformaldehyde for 20 min and stained with 0.1% crystal violet for 10 min. Under a light microscope (Olympus), the stained cells were photographed.

Methylated RNA immunoprecipitation (MeRIP)

The m6A level of circXPO1 was determined by MeRIP using the RIP kit (cat. no. 17-10499, Millipore, MA, USA). Cell lysates were extracted using the RIP lysis buffer. Then, 150 μg of total RNA was immunoprecipitated magnetic beads (MCE) pre-coated with 5 μg of anti-m6A (A19841, ABclonal, Wuhan, China) or anti-IgG (AC005, ABclonal) for 2 h at 4°C. The m6A-modified RNAs were eluted using proteinase K for 45 min at 55˚C. Then, the

enrichment of circXPO1 in extracted RNA was assessed by RT-qPCR. The primer sequences are as follows: forward 5'-TGGTGAATTGCTTATACCATGG-3' and reverse 5'- GTTCCTTGGAAGAATCTTCCAC-3'.

RNA pull-down assay

A biotin-labeled circXPO1 probe and the random control probe were synthesized by RiboBio (Guangzhou, China). RNA pull-down assay was conducted using the Pierce™ Magnetic RNA-protein pull-down kit (cat. no. 20164, Thermo Fisher). In short, 100 μL M-280 Streptavidin Dynabeads (Thermo Fisher Scientific, Inc.) were pre-coated with 100 nM biotinylated probe for 2 h. The lysates of CRC cells were incubated with probe-coated streptavidin-conjugated magnetic beads at 4˚C for 3 h. After elution and purification, the samples were subjected to Western blotting.

RNA immunoprecipitation (RIP) assay

The Magna RIP Kit (cat. no. 17–704, Millipore) was adopted to perform RIP assay. The protein A/G magnetic beads (MCE) were pre-coated with 5 μg of antibodies against IGF2BP1 (ab184305, Abcam, UK), IGF2BP2 (ab128175, Abcam), IGF2BP3 (ab177477, Abcam), FMRP (ab259335, Abcam), or IgG (AC005, ABclonal). Subsequently, cell lysates were incubated with the pre-coated magnetic beads at 4˚C for 12 h, followed by treatment with proteinase K for 45 min at 55˚C. Following RNA purification, circXPO1 and WWC2 enrichment was measured by RT-qPCR. IgG was used as a negative control to preclude nonspecific binding.

Nude mouse tumorigenicity assay

Six-week-old male BALB/C nude mice were provided by SJA Laboratory Animal Co., Ltd. (Changsha, China). After one week of adaptive feeding, the nude mice were subcutaneously injected with 1×10^6 CRC cells that were stably transfected with shcircXPO1 or WWC2 plasmid to establish the xenograft model ($n=6$ per group). The length and width of tumors were detected to calculate tumor volume (V=length × width^2/2). The mice were subjected to euthanasia 4 weeks after the injection, and the tumors were collected and weighed. For evaluation of in vivo liver metastasis, 1×10^6 CRC cells that were stably transfected with shcircXPO1 or WWC2 plasmid were injected into the distal tip of the spleen as previously described. The mice were euthanized at 25 days after the injection, and the livers were excised to observe and count the metastatic tumor nodules. All experimental procedures were approved by the Ethics Committee of School of Basic Medicine, Jiamusi University.

Immunohistochemistry staining

The tumors were fixed in 4% paraformaldehyde at room temperature for 24 h, embedded into paraffin, and cut into 5-μm sections, followed by dewaxing and rehydration. The sections were then subjected to antigen retrieval in a citrate-EDTA antigen retrieval solution (cat. no. P0083; Beyotime) for 30 min at 95–100˚C. Subsequently, endogenous peroxidase activity was blocked with 10% hydrogen peroxide for 10 min at room temperature. After blocking in 3% BSA for 1 h, the sections were probed with primary antibodies against WWC2 (A18668, 1:50, ABclonal) and Ki-67 (ab15580, 1:100, Abcam) at 4 ˚C overnight. Subsequently, the sections were incubated with a secondary antibody HRP Donkey Anti-Rabbit IgG (AS038, 1:500, ABclonal) for 30 min. After staining with 3,3′-diaminobenzidine and counterstaining with hematoxylin, the sections were examined under a microscope.

Hematoxylin and Eosin (HE) staining

The collected livers were embedded into paraffin and cut into 5-μm sections. After deparaffinization and rehydration with gradient concentrations of ethanol, the sections were subjected to hematoxylin (cat. no. G1120, Solarbio, Beijing, China) staining for 1 min, rinsed with water for 10 min, differentiated with hydrochloric acid ethanol for 3 s, and subsequent eosin staining (Solarbio) for 30 s. The liver sections were observed using the light microscope.

Quantitative reverse transcription PCR (RT-qPCR)

Cells and tumors were collected to isolate total RNAs using the TRIzol (cat. no. 12183555, Thermo Fisher), followed by reverse transcription to cDNA using the PrimeScript™RT reagent kit (cat. no. RR037A, Takara, Osaka, Japan). Then, RT-qPCR was conducted with the cDNA template using the 2×SYBR Green PCR Mastermix (cat. no. SR1110, Solarbio) to amplify the specific genes. The following thermocycling conditions were used for the qPCR: Initial denaturation at 95˚C for 3 min; followed by 40 cycles at 95˚C for 15 s, annealing at 60˚C for 30 s, elongation at 72˚C for 1 min; and a final extension at 72˚C for 5 min. The relative gene levels normalized to GAPDH were calculated by using the $2^{-\Delta\Delta CT}$ method. The primer sequences are listed in Table 1.

Western blotting

Total protein was extracted from CRC cells or tissues with the RIPA buffer (cat. no. R0010, Solarbio), and protein concentration was quantified by the BCA Protein Assay Kit (cat. no. PC0020, Solarbio). A total of 30 μg protein samples were separated by SDS-PAGE, blotted onto PVDF membranes, and blocked with 5% nonfat milk for 1 h at 25˚C. The membranes were incubated with primary antibodies against E-cadherin (A3044, 1:500, ABclonal), N-cadherin (A0432, 1:500,

Table 1 Primer sequences for RT-qPCR

Genes	Primer sequences (5′-3′)
circXPO1-F	GGAACCAGTGCGAAGTAATCT
circXPO1-R	GCTGAAATCAAGCAGCTGACG
WWC2-F	TTCATCCGCCCACAGAATCC
WWC2-R	AGCCAGGCATTCTTCCCTTC
IGF2BP2-F	TGGAAGCGCATATCAGAGTG
IGF2BP2-R	AGTGCCCGATAATTCTGACG
FMRP-F	TCAAGGCTTGGCAGGGTATG
FMRP-R	TCCTCTGTTGGAGCTTTAAATAGT
ALKBH5-F	ATTAGATGCACCCCGGTTGG
ALKBH5-R	GCCGGTTCTCTTCCTTGTCC
GAPDH-F	CCAGGTGGTCTCCTCTGA
GAPDH-R	GCTGTAGCCAAATCGTTGT

ABclonal), Vimentin (ab20346, 1:1000, Abcam), Snail (A11794, 1:1000, ABclonal), IGF2BP2 (ab128175, 1:1000, Abcam), WWC2 (A18668, 1:500, ABclonal), FMRP (ab259335, 1:1000, Abcam), p-YAP1 (ab76252, 1:1000, Abcam), YAP1 (A1002, 1:1000, ABclonal), p-LATS1/2 (AP1517, 1:500, ABclonal) and GAPDH (AC001, 1:10000, ABclonal) at 4 °C overnight. Then, incubation with horseradish peroxidase-conjugated secondary antibody (AS038, 1:5000, ABclonal) was performed for 1 h at 25°C. Finally, the signals were detected using the enhanced chemiluminescence system (cat. no. WP20005, Thermo Fisher) and quantified using the ImageLab software (version 2.3; Bio-Rad Laboratories, Inc.).

Statistical analysis

All data from three independent experiments are presented as mean±standard deviation (SD). Statistical significance was analyzed using Student's t test for two groups or one-way analysis of variance (ANOVA) followed by Tukey's post hoc test for more than three groups using GraphPad Prism 8.0 software. Survival analysis was performed using Kaplan-Meier analysis. The correlation between circXPO1 and WWC2 levels was analyzed by Spearman correlation analysis. $P<0.05$ was considered as statistically significant.

Results

Characterization of circXPO1 and its aberrant high expression in CRC

The circular structure of circXPO1 was evaluated by Sanger-sequencing. circXPO1 (circBase ID: hsa_circ_0001017) is a circRNA transcript generated by back-splicing of the 2–4 exons of the XPO1 gene (Fig. 1A). Moreover, circXPO1 level was not remarkably changed, while linear XPO1 level was declined ($P<0.01$) in CRC cells after exposure to RNase R, suggesting an intact circular structure of circXPO1 (Fig. 1B). In addition, circXPO1 exhibited a longer half-life after actinomycin D treatment in comparison with linear XPO1 (Fig. 1C, $P<0.05$ or $P<0.01$). More importantly, circXPO1 was mainly expressed in the cytoplasm (Fig. 1D&E). Furthermore, we detected the level of circXPO1 in 56 paired CRC and adjacent normal tissues. We found a higher level of circXPO1 in CRC tissues as compared with adjacent normal tissues (Fig. 1F, $P<0.01$). Furthermore, high expression of circXPO1 indicated a lower survival rate of CRC patients (Fig. 1G, $P=0.0078$). Additionally, circXPO1 was up-regulated in several CRC cell lines as compared with normal FHC cells, among which HCT116 ($P<0.001$) and SW480 ($P<0.001$) cells exhibited higher level of circXPO1 (Fig. 1H). To sum up, circXPO1 was highly expressed in CRC tissues and cells, which was correlated with a poor prognosis.

circXPO1 knockdown represses growth, metastasis, and epithelial-mesenchymal transition (EMT) of CRC cells

To explore the influence of circXPO1 on malignant capacities of CRC cells, circXPO1 was knocked down in HCT116 and SW480 cells by transfection with shcircXPO1 (Fig. 2A, $P<0.01$). Colony formation assay showed that the growth of CRC cells was delayed after circXPO1 knockdown (Fig. 2B, $P<0.01$). Subsequently, scratch and transwell assays demonstrated that the migration and invasion were repressed in circXPO1-silenced CRC cells (Fig. 2C&D, $P<0.05$ or $P<0.01$). Moreover, down-regulation of circXPO1 inhibited EMT process as confirmed by increasing E-cadherin expression ($P<0.001$ or $P<0.01$) and reducing N-cadherin ($P<0.01$), Vimentin ($P<0.05$ or $P<0.001$) and Snail ($P<0.05$ or $P<0.001$) expression (Fig. 2E). These findings suggested that circXPO1 deficiency inhibited the malignant phenotypes of CRC cells.

ALKBH5 inhibits circXPO1 expression via IGF2BP-m6A modification

m6A modification, a frequent RNA modification, plays key roles in the biogenesis and function of circRNAs. To further investigate the influence of m6A modification on the dysregulation of circXPO1 in CRC, the m6A level of circXPO1 was measured in a series of CRC cell lines. As assessed by MeRIP, the m6A level of circXPO1 was strikingly enhanced in various CRC cells (Fig. 3A, $P<0.01$ or $P<0.001$). Additionally, the regulation of m6A methyltransferases (METTL3, METTL14) and demethylases (ALKBH5, FTO) in circXPO1 expression was detected. circXPO1 expression was only reduced by ALKBH5 overexpression in CRC cells ($P<0.01$), but not affected by METTL3, METTL14, or FTO overexpression (Fig. 3B). Besides, MeRIP assay demonstrated that the m6A level of circXPO1 was evidently declined in ALKBH5-overexpressed cells (Fig. 3C, $P<0.01$ or $P<0.001$). RIP assay further revealed that circXPO1 could be enriched by methylation reading proteins, including IGF2BP1,

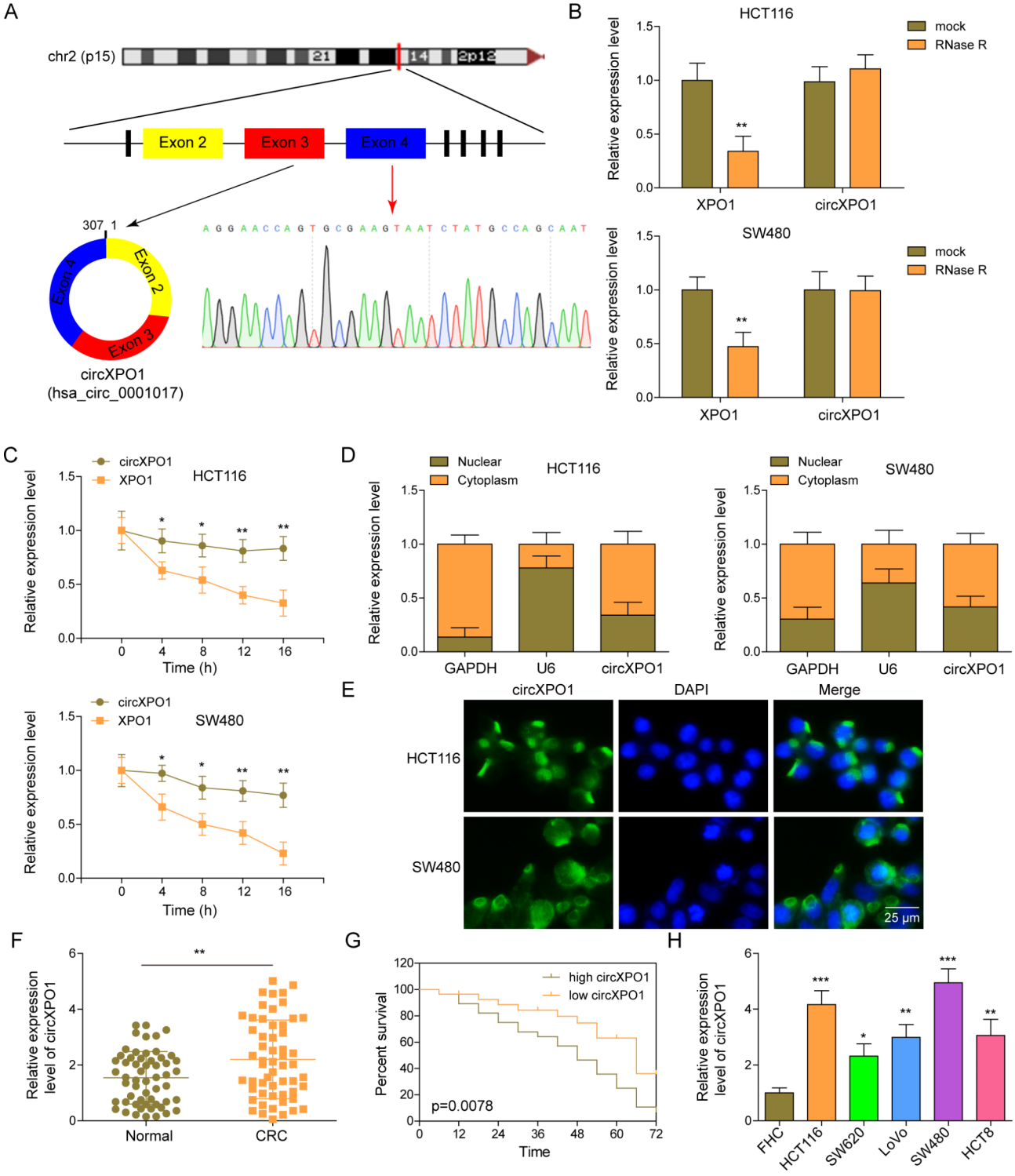

Fig. 1 circXPO1 was up-regulated in CRC and associated with a poor prognosis. (**A**) circXPO1 is formed by circularization of exons 2–4 of XPO1 gene. The back-splicing junctions of circXPO1 was confirmed by Sanger sequencing. (**B**)&(**C**) circXPO1 and linear XPO1 levels were assessed by RT-qPCR. (**D**) RT-qPCR analysis of circXPO1 expression in the cytoplasmic and nuclear fractions of CRC cells. (**E**) FISH assay identified the subcellular expression of circXPO1 in CRC cells (scale bar = 25 μm). (**F**) circXPO1 level in CRC and normal tissues was measured by RT-qPCR. (**G**) Kaplan-Meier analysis of survival of parents with high or low expression of circXPO1. (**H**) circXPO1 expression in CRC cells and normal FHC cells was detected by RT-qPCR. The results from three independent experiments are displayed as the mean ± SD. Student's t test (for **B**, **C**, **F**) and one-way ANOVA (for H) were performed for statistical analysis. **P* < 0.05; ***P* < 0.01; ****P* < 0.001

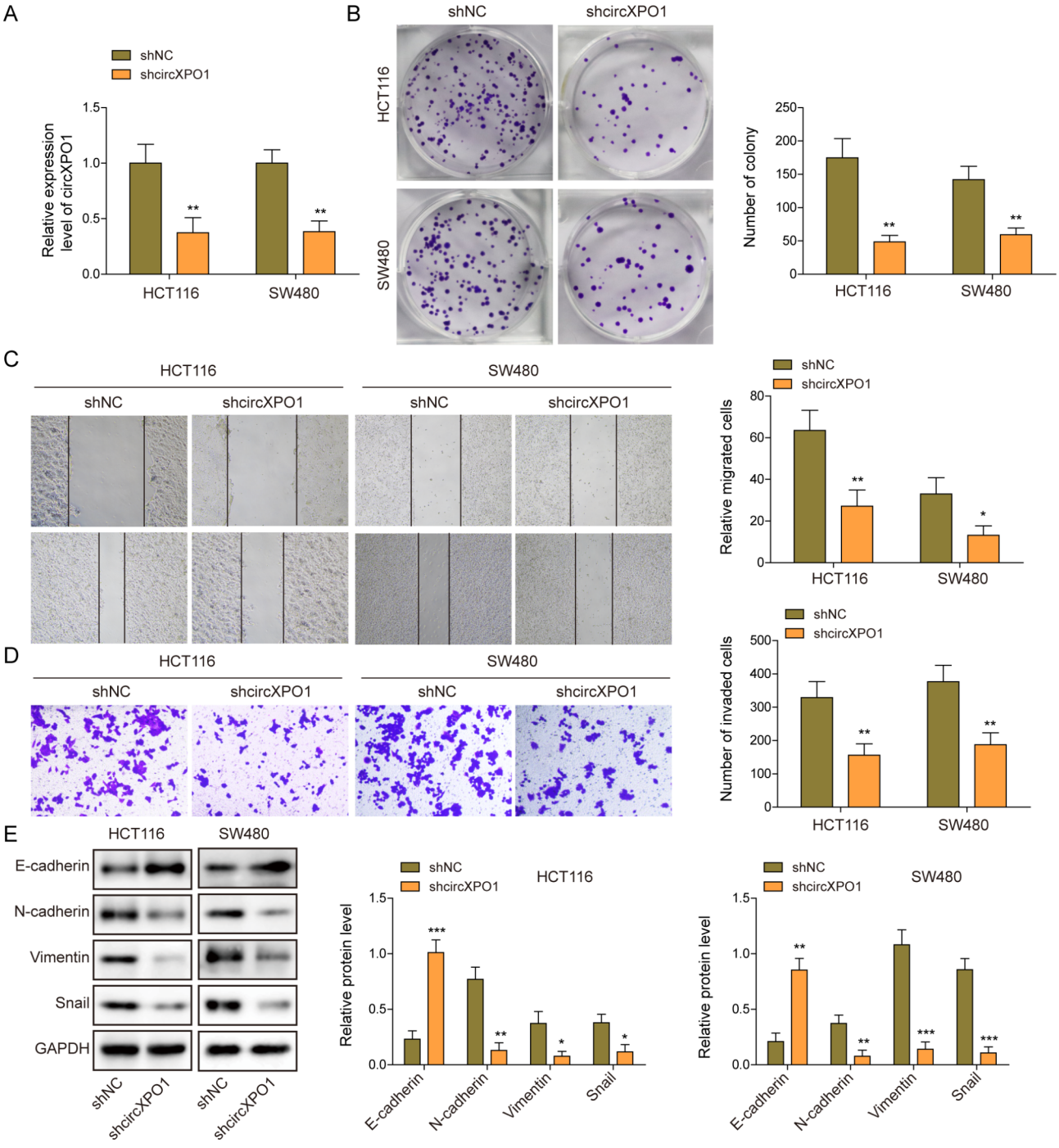

Fig. 2 circXPO1 deficiency suppressed the growth, metastasis and EMT of CRC cells. CRC cells were stably transfected with shcircXPO1 or shNC. (**A**) circXPO1 level in CRC cells transfected with shcircXPO1 was evaluated by RT-qPCR. (**B**) CRC cell growth was determined by colony formation assay. (**C**) Scratch assay determined CRC cell migration. (**D**) The invasive capacity was assessed by Transwell assay. (**E**) E-cadherin, N-cadherin, Vimentin, and Snail protein abundance was detected by Western blotting. The results from three independent experiments are displayed as the mean ± SD. Student's t test was performed for statistical analysis. *$P < 0.05$; **$P < 0.01$; ***$P < 0.001$

IGF2BP2, IGF2BP3. Among which the enrichment level of circXPO1 was highest after immunoprecipitation with IGF2BP2 antibody (Fig. 3D, $P<0.001$). Thus, IGF2BP2 was selected in the subsequent experiments. To investigate the modulation of IGF2BP2 in circXPO1 expression, IGF2BP2 was overexpressed in CRC cells by transfection with IGF2BP2 overexpression plasmid (Fig. 3E&F, $P<0.05$, $P<0.01$or $P<0.001$). The stability of circXPO1 in CRC cells upon actinomycin D exposure was reduced by ALKBH5 overexpression ($P<0.01$), which was recovered

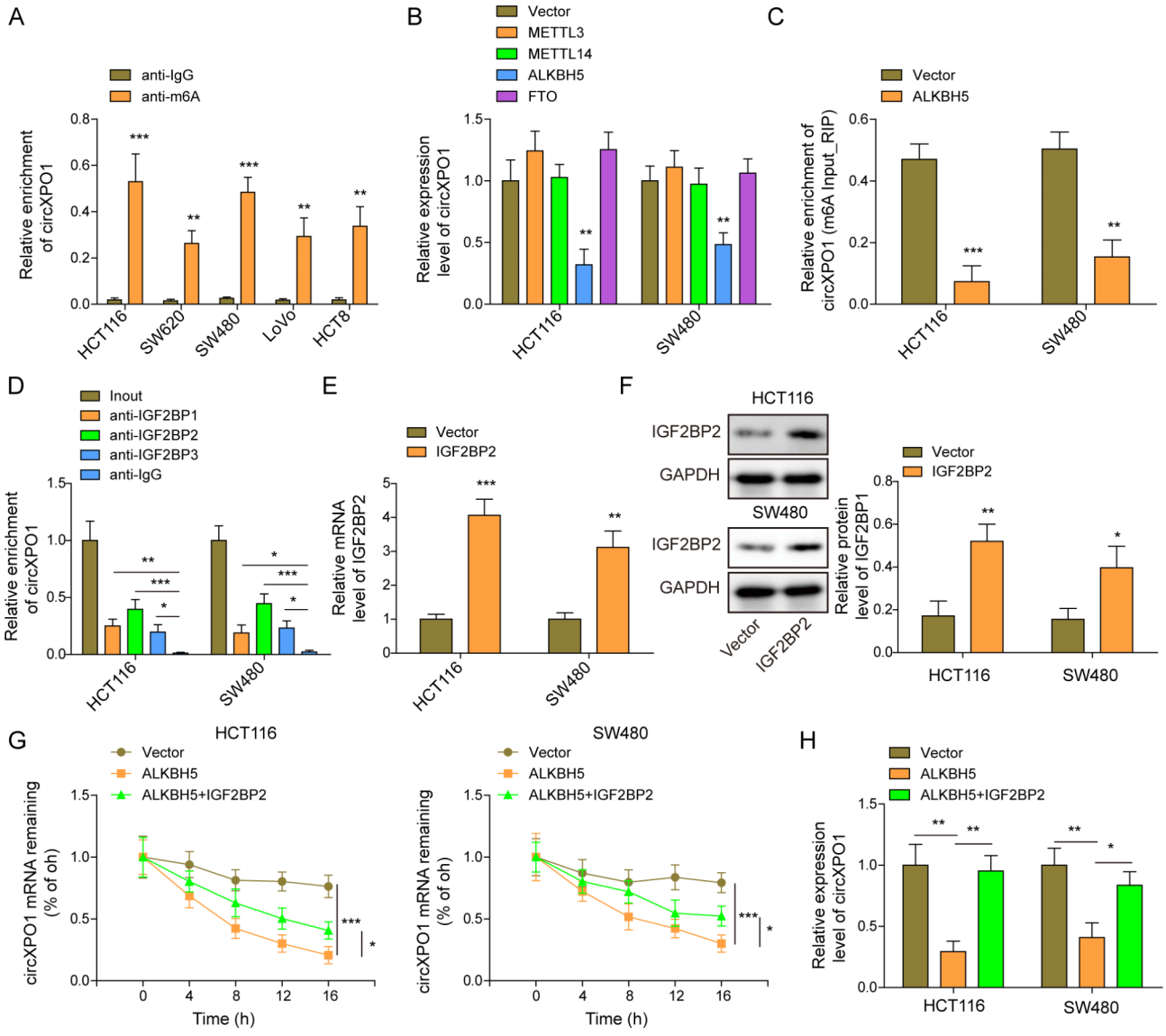

Fig. 3 ALKBH5 inhibited circXPO1 expression through repressing IGF2BP-mediated m6A modification. (**A**) circXPO1 m6A level in various CRC cells was analyzed by MeRIP. (**B**) CRC cells were transfected with ALKBH5, METTL3, METTL14, or FTO overexpression plasmid, and circXPO1 expression was detected by RT-qPCR. (**C**) MeRIP analysis of circXPO1 m6A level in CRC cells transfected with ALKBH5 overexpression plasmid. (**D**) The interplay between circXPO1 and IGF2BP1/2/3 was evaluated by RIP assay. (**E**)&(**F**) CRC cells were transfected with IGF2BP2 overexpression plasmid, and IGF2BP2 expression was assessed by RT-qPCR and Western blotting. CRC cells were transfected with ALKBH5 overexpression plasmid combined with or without IGF2BP2 overexpression plasmid. (**G**) circXPO1 stability was determined by RT-qPCR. (**H**) circXPO1 level was analyzed by RT-qPCR. The results from three independent experiments are displayed as the mean ± SD. Student's t test (for **A**, **C**, **E**, **F**) and one-way ANOVA (for **B**, **D**, **G**, **H**) were performed for statistical analysis. *$P < 0.05$; **$P < 0.01$; ***$P < 0.001$

by IGF2BP2 overexpression ($P<0.05$) (Fig. 3G). Besides, circXPO1 expression was reduced by ALKBH5 overexpression ($P<0.01$), which was reversed after co-transfection with IGF2BP2 overexpression plasmid ($P<0.05$ or $P<0.01$) (Fig. 3H). Collectively, the above findings suggested that ALKBH5 restrained circXPO1 expression via inhibiting IGF2BP2-mediated m6A modification.

circXPO1 promotes WWC2 mRNA degradation via interaction with FMRP

Next, we sought to explore the downstream mechanism through which circXPO1 contributed to the malignant capacities of CRC cells. GEPIA2 database indicated that WWC2 was lowly expressed in colonic adenocarcinoma (COAD) and rectum adenocarcinoma (READ) samples (Fig. 4A, $P<0.05$). Consistently, our data revealed that WWC2 expression was declined in CRC tissues, which was negatively correlated with circXPO1 level (Fig. 4B-D,

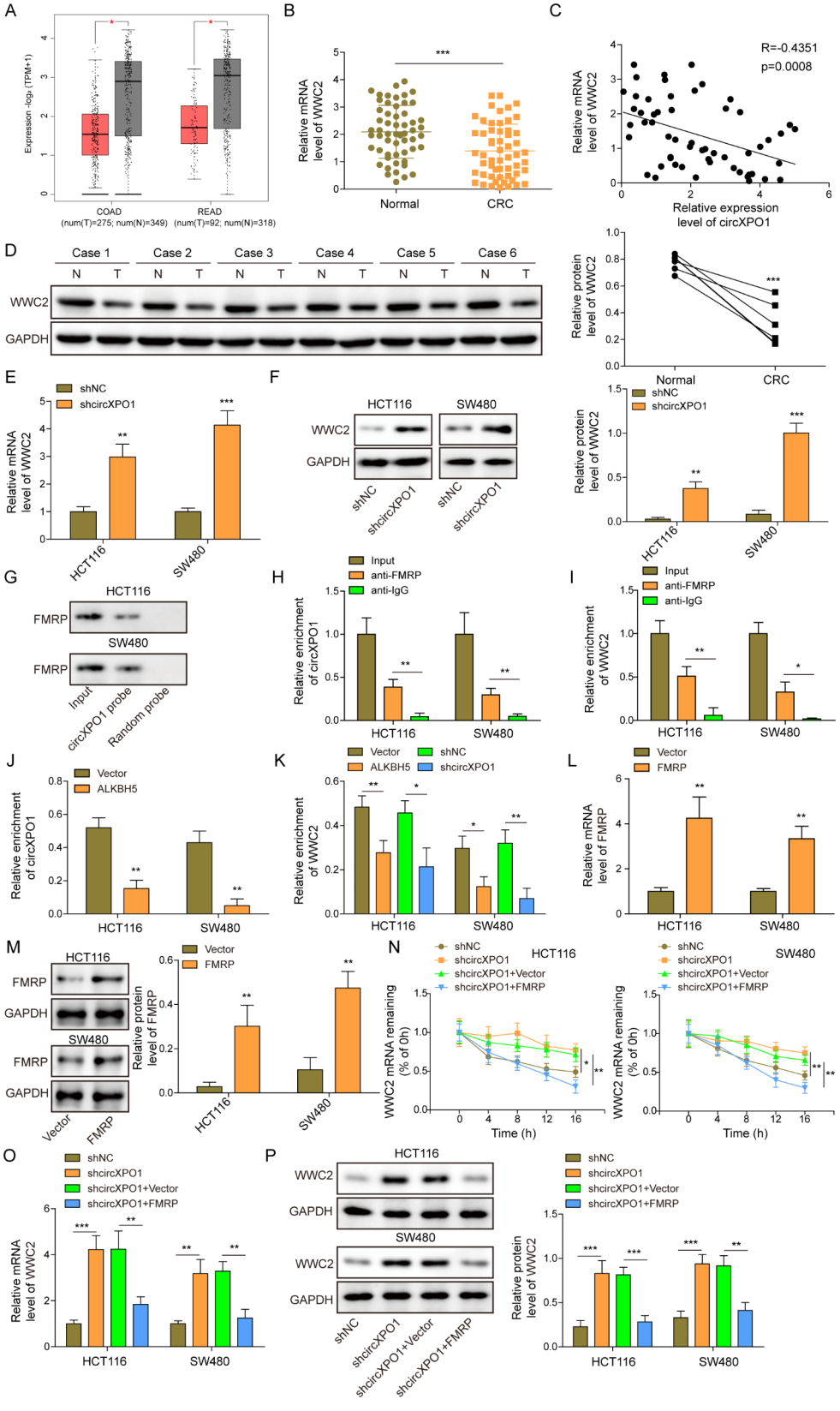

Fig. 4 (See legend on next page.)

(See figure on previous page.)

Fig. 4 circXPO1 directly interacted with FMRP to cause WWC2 mRNA degradation. (**A**) GEPIA2 database analyzed WWC2 expression in colonic adenocarcinoma (COAD) and rectum adenocarcinoma (READ) samples. (**B**) RT-qPCR measured WWC2 expression in CRC samples and paired normal tissues. (**C**) Correlation between circXPO1 and WWC2 was analyzed by Spearman correlation analysis. (**D**) WWC2 protein level in paired CRC and normal tissues was determined by Western blotting. (**E**) &(**F**) WWC2 expression in shcircXPO1-transfected CRC cells were measured by RT-qPCR and Western blotting. (**G**) The binding of circXPO1 to FMRP was analyzed by RNA pull-down assay. (**H**)&(**I**) The interaction between FMRP and circXPO1/WWC2 was confirmed by RIP assay. (**J**) The interaction between FMRP and circXPO1 after ALKBH5 overexpression was evaluated by RIP assay. (**K**) The binding of FMRP to WWC2 in CRC cells transfected with ALKBH5 overexpression plasmid or shcircXPO1 was determined by RIP assay. (**L**)&(**M**) FMRP expression in CRC cells transfected with FMRP overexpression plasmid were assessed by RT-qPCR and Western blotting. CRC cells were transfected with shcircXPO1 together with FMRP overexpression plasmid. (**N**) WWC2 mRNA stability was analyzed by RT-qPCR. (**O**)&(**P**) WWC2 expression was assessed by RT-qPCR and Western blotting. The results from three independent experiments are displayed as the mean ± SD. Student's t test (for A, B, D-F, J-M) and one-way ANOVA (for G-I, N-P) were performed for statistical analysis. *$P<0.05$; **$P<0.01$; ***$P<0.001$

$P<0.001$). Furthermore, silencing of circXPO1 led to an elevation in WWC2 expression in CRC cells (Fig. 4E&F, $P<0.01$ or $P<0.001$). Notably, RNA pull-down assay proved that circXPO1 could bind to RNA binding protein FMRP (Fig. 4G). Additionally, both circXPO1 and WWC2 could directly bind to FMRP protein (Fig. 4H&I, $P<0.01$ or $P<0.05$). RIP results showed that ALKBH5 overexpression reduced the interaction between circXPO1 and FMRP (Fig. 4J, $P<0.01$). In addition, the binding of FMRP to WWC2 was weakened by ALKBH5 overexpression or circXPO1 silencing (Fig. 4K, $P<0.05$ or $P<0.01$). As illustrated in Fig. 4L&M, FMRP expression was elevated in FMRP-overexpressed CRC cells ($P<0.01$). In addition, circXPO1 deficiency restrained actinomycin D-induced degradation of WWC2 mRNA ($P<0.01$ or $P<0.05$), whereas this effect was neutralized by FMRP overexpression ($P<0.01$) (Fig. N). Furthermore, WWC2 level was elevated by circXPO1 knockdown ($P<0.001$ or $P<0.01$), which was reversed by FMRP overexpression ($P<0.001$ or $P<0.01$) (Fig. 4O&P). Collectively, we demonstrated that circXPO1 silencing disrupted the interaction between FMRP and WWC2 to promote WWC2 mRNA degradation.

WWC2 overexpression suppresses CRC cell growth, metastasis, EMT and Hippo-YAP signaling

Given that WWC2 was a downstream target of circXPO1, we further elucidated the regulation of WWC2 in malignant development of CRC. For this purpose, WWC2 was overexpressed in CRC cells after transfection with WWC2 overexpression plasmid (Fig. 5A&B, $P<0.001$ or $P<0.01$). Functional experiments revealed that WWC2 overexpression distinctly suppressed the growth, migration, and invasion of CRC cells (Fig. 5C-E, $P<0.05$ or $P<0.01$). Besides, E-cadherin was up-regulated ($P<0.001$), while N-cadherin ($P<0.01$), Vimentin ($P<0.001$ or $P<0.01$), and Snail ($P<0.001$ or $P<0.01$) were down-regulated in CRC cells after WWC2 overexpression, indicating the inhibition of EMT (Fig. 5F). We next investigated the involvement of Hippo-YAP signaling pathway in the anti-tumor effects of WWC2 in CRC cells. We found that the levels of p-YAP1 ($P<0.001$ or $P<0.01$) and p-LATS1/2 ($P<0.01$) were elevated by overexpression of WWC2 in CRC cells (Fig. 5G), indicating the inactivation of Hippo pathway. These findings revealed that WWC2 overexpression inactivated Hippo-YAP pathway and restrained the function of CRC cells.

circXPO1 triggers CRC cell growth and metastasis via regulation of the WWC2/Hippo-YAP axis

To validate the regulation of circXPO1/WWC2 axis in CRC progression, CRC cells were transfected with circXPO1 overexpression plasmid together with or without WWC2 overexpression plasmid. CircXPO1 overexpression efficiency was confirmed by RT-qPCR (Fig. 6A, $P<0.001$ or $P<0.01$). The levels of p-YAP1 and p-LATS1/2 were reduced by circXPO1 overexpression ($P<0.001$, $P<0.01$ or $P<0.05$), which were recovered by WWC2 overexpression ($P<0.001$ or $P<0.01$) (Fig. 6B). In addition, circXPO1 overexpression exerted promotive effects on CRC cell growth, migration, and invasion, whereas these changes were counteracted by WWC2 overexpression or treatment with verteporfin, an inhibitor of Hippo pathway (Fig. 6C-E, $P<0.001$, $P<0.01$ or $P<0.05$). Furthermore, the decreased E-cadherin expression and elevated N-cadherin, Vimentin and Snail levels in circXPO1-overexressed CRC cells were reversed by WWC2 overexpression or co-treatment with verteporfin (Fig. 6F, $P<0.001$, $P<0.01$ or $P<0.05$). Therefore, circXPO1 facilitated WWC2 mRNA decay to confer the growth and metastasis of CRC cells via activating the Hippo-YAP pathway.

circXPO1 deficiency or WWC2 overexpression delays CRC growth and metastasis in vivo

To validate the above results in vivo, the nude mice were subcutaneously injected with CRC cells stably transfected with shcircXPO1 or WWC2 overexpression plasmid. We observed that the tumor volume and weight were lower in circXPO1 silencing or WWC2 overexpression group in comparison with the shNC or vector group (Fig. 7A-C, $P<0.001$ or $P<0.01$). circXPO1 depletion or WWC2 overexpression strikingly enhanced WWC2 mRNA level in the tumors (Fig. 7D, $P<0.001$ or $P<0.01$). Western blotting data indicated that the protein levels of WWC2, p-YAP1, p-LATS1/2 and E-cadherin were up-regulated,

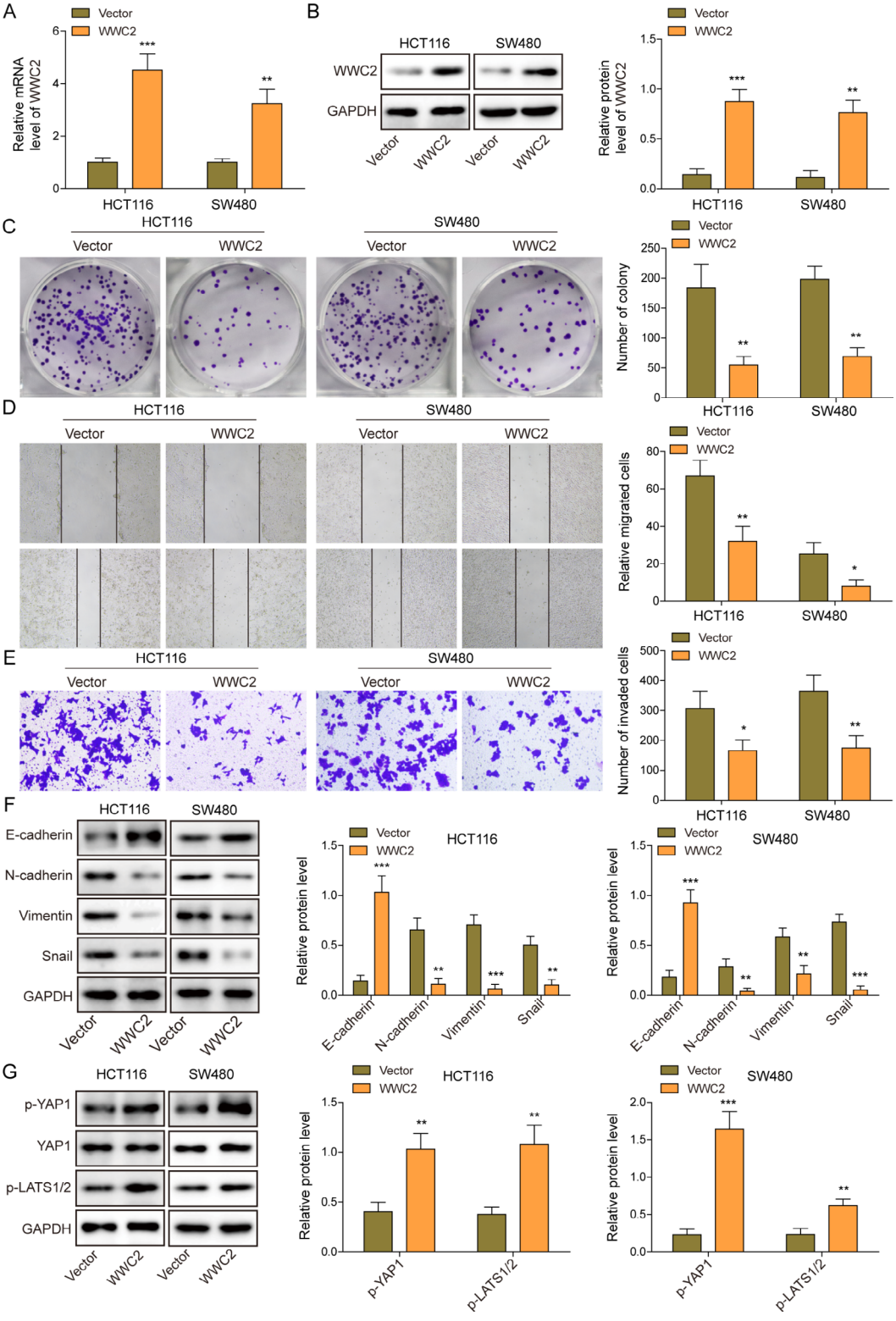

Fig. 5 WWC2 overexpression inhibited the malignant capacities of CRC cells and Hippo-YAP signaling. CRC cells were stably transfected with WWC2 overexpression plasmid or vector. (**A**)&(**B**) WWC2 expression in CRC cells was evaluated by RT-qPCR and Western blotting. (**C**) CRC cell growth was evaluated by colony formation assay. (**D**) Scratch assay analyzed the migration of CRC cells. (**E**) The invasion was assessed by Transwell assay. (**F**)&(**G**) E-cadherin, N-cadherin, Vimentin, Snail, p-YAP1, YAP1 and p-LATS1/2 protein abundance was analyzed by Western blotting. The results from three independent experiments are displayed as the mean ± SD. Student's t test was performed for statistical analysis. *$P < 0.05$; **$P < 0.01$; ***$P < 0.001$

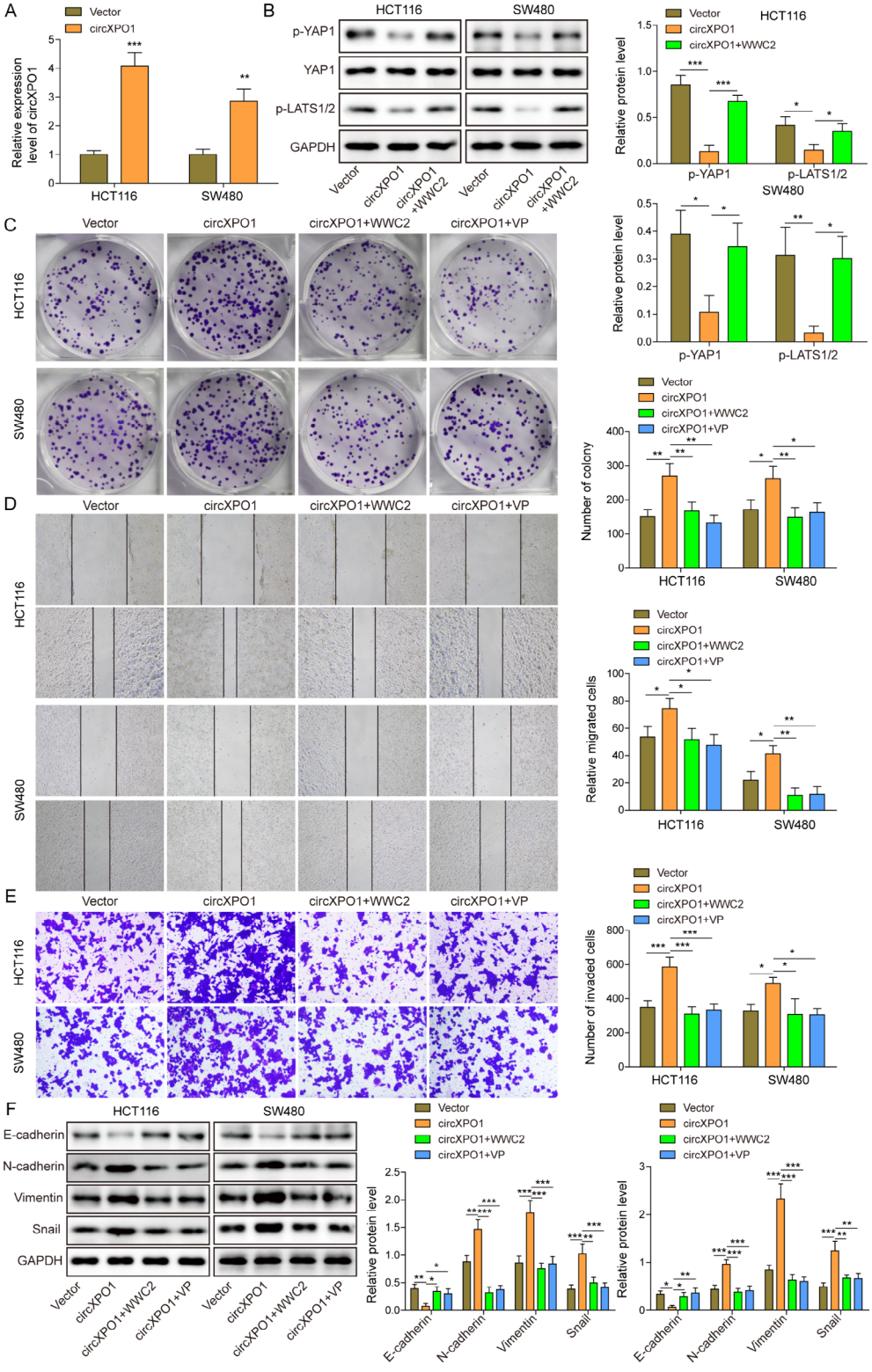

Fig. 6 circXPO1 destabilized WWC2 to facilitate CRC cell growth and metastasis via activating Hippo-YAP pathway. CRC cells were transfected with circXPO1 overexpression plasmid combined with WWC2 overexpression plasmid or co-treatment with verteporfin (VP). (**A**) The overexpression efficiency of circXPO1 was verified by RT-qPCR. (**B**) Protein levels of p-YAP1, YAP1 and p-LATS1/2 were assessed by Western blotting. (**C**) CRC cell growth was evaluated by colony formation assay. (**D**) CRC cell migration was measured by scratch assay. (**E**) The invasive capacity was determined by Transwell assay. (**F**) E-cadherin, N-cadherin, Vimentin, and Snail protein abundance was assessed by Western blotting. The results from three independent experiments are displayed as the mean ± SD. Student's t test (for A) and one-way ANOVA (for B-F) were performed for statistical analysis. *$P < 0.05$; **$P < 0.01$; ***$P < 0.001$

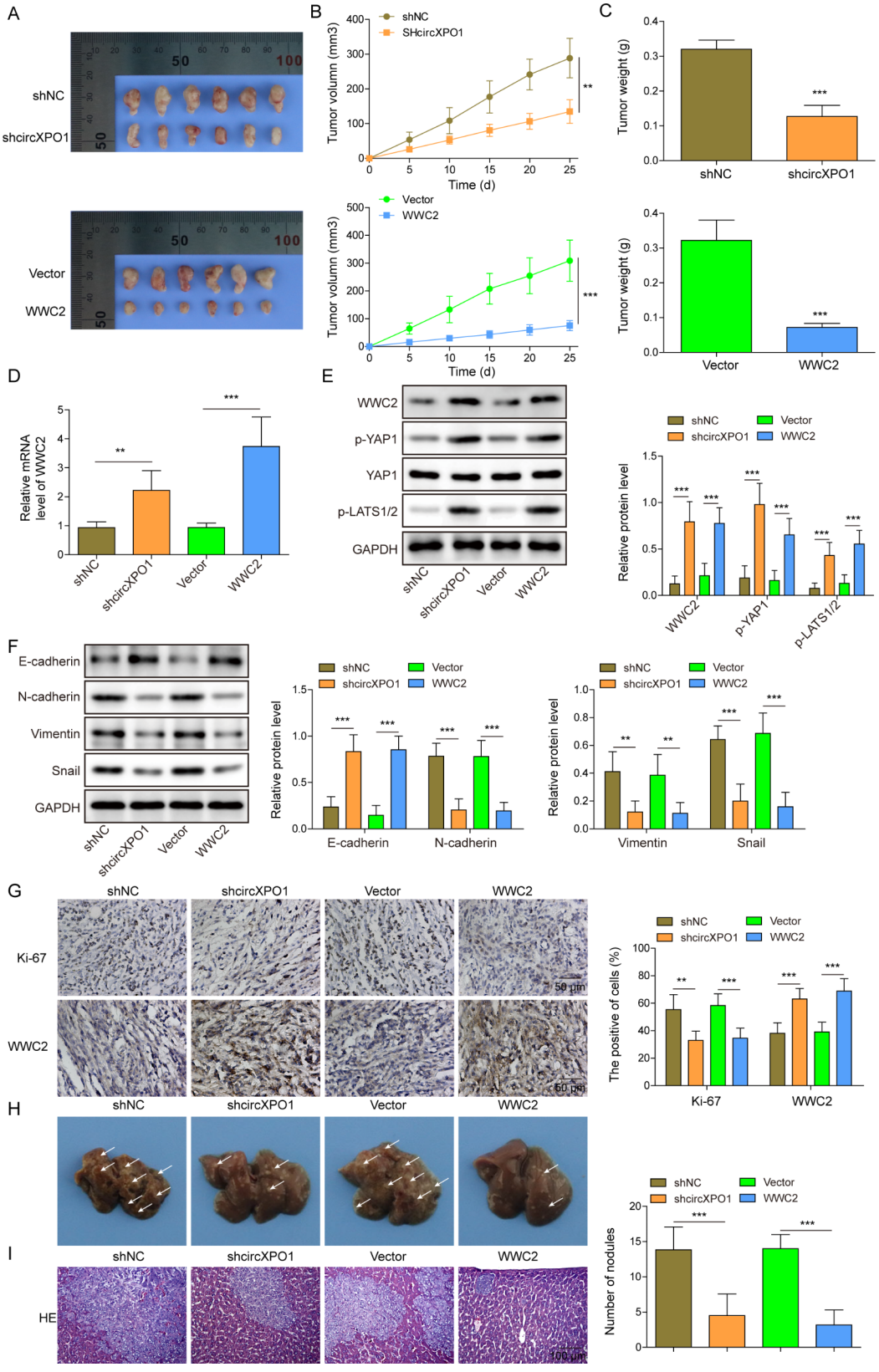

Fig. 7 (See legend on next page.)

(See figure on previous page.)

Fig. 7 circXPO1 deficiency or WWC2 overexpression restrained CRC growth and metastasis in vivo. (**A**) Images of xenograft tumors after subcutaneous injection with CRC cells transfected with shcircXPO1 or WWC2 overexpression plasmid. (**B**) The xenograft tumor volume was recorded. (**C**) The xenograft tumor weight was weighed at the endpoint time. (**D**) WWC2 mRNA level in tumors was detected by RT-qPCR. (**E**)&(**F**) WWC2, p-YAP1, YAP1, p-LATS1/2, E-cadherin, N-cadherin, Vimentin, and Snail protein levels were determined by Western blotting. (**G**) Immunohistochemical staining detected WWC2 and Ki-67 expression in tumor tissues (scale bar = 50 μm). (**H**) Images of liver metastasis model after injection with CRC cells transfected with shcircXPO1 or WWC2 overexpression plasmid. (**I**) The metastatic nodules in the livers were observed by HE staining (scale bar = 100 μm). The results are displayed as the mean ± SD ($n = 6$ per group). One-way ANOVA was performed for statistical analysis. $^{**}P < 0.01$; $^{***}P < 0.001$

while the protein levels of N-cadherin, Vimentin and Snail were down-regulated by circXPO1 deficiency or WWC2 overexpression (Fig. 7E&F, $P<0.001$ or $P<0.01$). Furthermore, immunohistochemistry staining showed that Ki-67 expression was decreased and WWC2 expression was increased in circXPO1-silenced or WWC2-overexpressed tumors (Fig. 7G, $P<0.001$ or $P<0.01$). Furthermore, the number of liver metastatic nodules was reduced in shcircXPO1 or WWC2 overexpression group (Fig. 7H&I, $P<0.001$). Collectively, our data suggested that circXPO1 knockdown or WWC2 overexpression delayed CRC progression by inactivation of the Hippo-YAP pathway.

Discussion

Although improvements have been made in therapies for CRC, the outcomes of CRC patients are still poor. Thus, there is an urgent need for the identification of novel effective therapeutic targets for CRC. Recent evidence has discovered the high expression of circXPO1 and its oncogenic role in various cancers [10, 24]. However, the influence of circXPO1 in CRC has not been reported. This work for the first time explored the biological function of circXPO1 in CRC. circXPO1 was found to be highly expressed in CRC patients, which indicated a poor prognosis. Functional experiments demonstrated that circXPO1 ablation delayed the growth, migration, invasion, and EMT of CRC cells. Mechanistically, ALKBH5 down-regulation enhanced circXPO1 expression via promoting IGF2BP-mediated m6A modification. circXPO1 interacted with FMRP to reduce WWC2 mRNA stability, which consequently led to activation of Hippo-YAP pathway. Our findings provide new insight into the oncogenic action of circXPO1 and its regulatory mechanisms in CRC.

Recently, circRNAs have been demonstrated to participate in the tumorigenesis and development of CRC. Besides, circRNAs have been considered as biomarkers for CRC due to the high stability [26]. circXPO1, a newly identified circRNA, is derived from XPO1 gene, which has been considered as a therapeutic target for tumor [24]. Up-regulation of circXPO1 has been found in various malignancies, such as prostate cancer [12], osteosarcoma [27], and so on. In line with these previous studies, our data showed high expression of circXPO1 in CRC, which suggested a lower survival of CRC patients. Furthermore, circXPO1 ablation exerted anti-cancer roles as evidenced by restraining CRC cell growth, metastasis, and EMT. Our observations provided first evidence that circXPO1 might be a diagnostic and therapeutic biomarker for CRC.

Next, we investigated the upstream regulatory mechanism of circXPO1 in CRC. m6A modification is one of frequent epigenetic modifications of RNAs. The splicing, translation, and stability of circRNAs have been recognized to be regulated by m6A modification [28]. Notably, our results showed that the m6A level of circXPO1 was evidently enhanced in CRC cells, suggesting the potential regulation of circXPO1 by m6A modification. ALKBH5, the m6A eraser, has been documented to delay CRC progression via regulation of m6A modification [29]. Another study also reported the anti-cancer effect of ALKBH5 on CRC, and lower ALKBH5 expression suggested a worse prognosis of CRC patients [15]. As an m6A reader, IGF2BP2 is responsible for the recognition of m6A modification [30]. Ye et al., documented that ALKBH5 delayed CRC development by suppressing HK2 expression via inhibiting IGF2BP2-mediated m6A modification [31]. Another study suggested that IGF2BP2 promoted aerobic glycolysis and progression of CRC by stabilizing m6A-modified GLUT1 mRNA [32]. In this work, we provided first evidence that low expression of ALKBH5 increased circXPO1expression in CRC cells by m6A modification in an IGF2BP2-dependent manner.

Although our findings have verified the oncogenic role of circXPO1 in CRC, its possible molecular mechanism remains largely unknown. Previous studies have suggested that circRNAs can modulate the malignant behaviors of cancers via direct interaction with RBPs [33, 34]. FMRP is an RBP that can affect mRNA stability of its targets [35]. A previous study documented that circZNF609 destabilized RAC1 mRNA via binding to FMRP, thus inhibiting melanoma metastasis [36]. So far, whether circXPO1 can interact with FMRP to regulate the malignant capacities of CRC cells remains unknown. Herein, our data for the first time indicated that circXPO1 directly interplayed with FMRP to degrade WWC2 mRNA in CRC cells. WWC2, a member of the WWC family, is an upstream regulator of Hippo signaling pathway, which can negatively regulate Hippo signaling pathway by direct binding to LATS1/2 via their WW domains to phosphorylate and activate LATS1/2, and consequently leads to phosphorylation of YAP to prevent its nuclear translocation [20]. Yuan et al., reported that WWC2 was lowly

expressed in CRC, which was involved in LINC00460-induced metastasis of CRC cells [22]. Although WWC2-mediated CRC metastasis has been confirmed, whether WWC2 affected CRC development via regulation of Hippo-YAP pathway has not been clarified. Herein, our findings suggested that circXPO1 facilitated WWC2 mRNA decay to trigger Hippo-YAP pathway activation, thus accelerating the progression of CRC. This is the first study to explore the clinical relevance of circXPO1 expression regulated by ALKBH5/IGF2BP2 axis and its downstream target WWC2 in CRC patients. We observed a significant increase of circXPO1 expression and a reduction in WWC2 expression in tumor tissues from CRC patients. Our data from clinical specimens implied that circXPO1 might serve as a diagnostic and/or treatment target for CRC patients.

However, there are still some limitations in this study. First, we recognize that circXPO1 may exert biological functions via other mechanisms beyond binding to RBPs, such as serving as sponges of miRNAs to modulate the activity of miRNAs on their target genes. Additional mechanisms should be explored to fully elucidate whether circXPO1 modulated WWC2 via sponging miRNAs. Second, more investigation is needed to validate the applicability of our findings to clinical patients. In the future, we will strengthen the study on clinical relevance, clinical diagnostic and therapeutic targets.

Conclusions

In summary, circXPO1 was up-regulated in CRC, which conferred malignant capacities of CRC cells. Mechanistically, low expression of ALKBH5 enhanced circXPO1 expression via promoting IGF2BP2-dependent m6A modification, which subsequently destabilized WWC2 mRNA via binding to FMRP to activate Hippo-YAP pathway. These observations offer a potential therapeutic target, circXPO1, to broaden the treatment options for CRC patients.

Abbreviations

CRC	colorectal cancer
circRNAs	circular RNAs
m6A	N6-methyladenosine
ALKBH5	AlkB homolog 5,RNA demethylase
WWC2	WW and C2 domain containing 2
FMRP	fragile X mental retardation protein
shcircXPO1	short hairpin RNA targeting circXPO1
FISH	fluorescence in situ hybridization
MeRIP	methylated RNA immunoprecipitation
RIP	RNA immunoprecipitation
HE	Hematoxylin and Eosin
RT-qPCR	quantitative reverse transcription PCR
SD	standard deviation
ANOVA	analysis of variance
EMT	epithelial-mesenchymal transition
COAD	colonic adenocarcinoma
READ	rectum adenocarcinoma

Acknowledgements

None.

Author contributions

Xiaowen Zhu and Pengxia Zhang developed the manuscript concept. Xiaowen Zhu performed statistical analyses in original reports and Pengxia Zhang wrote the manuscript. All authors critically revised the manuscript for important intellectual content and approved the final version.

Funding

This work was supported by Heilongjiang Provincial Department of Education basic scientific research business expenses personnel training project (No.2017-KYYWF-0580) for Xiaowen Zhu, Northern medicine and functional food characteristic subject of Heilongjiang Province second project (LJGXCG02023-089) for Pengxia Zhang, Heilongjiang Province "double first-class" discipline collaborative innovation achievement project (No. LJGXCG02023-089) for Pengxia Zhang, The national science and technology ministry high-end foreign experts introduce the plan (No.G2022011018L) for Pengxia Zhang and Jiamusi University East Pole Academic Team (DJXSTD202404)for Pengxia Zhang.

Data availability

All data generated or analyzed during this study are included in this published article.

Declarations

Ethics approval and consent to participate

The Ethics Committee of School of Basic Medicine, Jiamusi University approved the study.
All experimental procedures were approved by the Ethics Committee of School of Basic Medicine, Jiamusi University.

Consent for publication

Not applicable.

Competing interests

The authors declare that they have no conflict of interest.

Received: 29 July 2024 / Accepted: 2 October 2024
Published online: 14 October 2024

References

1. Sung H, Ferlay J, Siegel RL, Laversanne M, Soerjomataram I, Jemal A, et al. Global Cancer statistics 2020: GLOBOCAN estimates of incidence and Mortality Worldwide for 36 cancers in 185 countries. CA Cancer J Clin. 2021;71(3):209–49.
2. Hofheinz RD, Stintzing S. Study evidence confirms current clinical practice in refractory metastatic colorectal cancer: the ReDOS trial. Lancet Oncol. 2019;20(8):1036–7.
3. Chen B, Hong Y, Gui R, Zheng H, Tian S, Zhai X, et al. N6-methyladenosine modification of circ_0003215 suppresses the pentose phosphate pathway and malignancy of colorectal cancer through the miR-663b/DLG4/G6PD axis. Cell Death Dis. 2022;13(9):804.
4. Dekker E, Tanis PJ, Vleugels JLA, Kasi PM, Wallace MB. Colorectal cancer. Lancet. 2019;394(10207):1467–80.
5. Shu H, Zhang Z, Liu J, Chen P, Yang C, Wu Y et al. Circular RNAs: an emerging precise weapon for diabetic nephropathy diagnosis and therapy. Biomed Pharmacother. 2023; 168115818.
6. Goodall GJ, Wickramasinghe VO. RNA in cancer. Nat Rev Cancer. 2021;21(1):22–36.
7. Zhang Y, Luo J, Yang W, Ye WC. CircRNAs in colorectal cancer: potential biomarkers and therapeutic targets. Cell Death Dis. 2023;14(6):353.
8. Yuan M, Zhang X, Yue F, Zhang F, Jiang S, Zhou X et al. CircNOLC1 Promotes Colorectal Cancer Liver Metastasis by Interacting with AZGP1 and Sponging miR-212-5p to Regulate Reprogramming of the Oxidative Pentose Phosphate Pathway. Adv Sci (Weinh). 2023e2205229.

9. Chen Z, Cheng H, Zhang J, Jiang D, Chen G, Yan S, et al. Hsa_circRNA_102051 regulates colorectal cancer proliferation and metastasis by mediating Notch pathway. Cancer Cell Int. 2023;23(1):230.
10. Li F, Liu J, Miao J, Hong F, Liu R, Lv Y, et al. Circular RNA circXPO1 promotes multiple myeloma progression by regulating miR-495-3p/DNA damage-Induced transcription 4 Axis. DNA Cell Biol. 2024;43(1):39–55.
11. Wang X, Wang J, An Z, Yang A, Qiu M, Tan Z. CircXPO1 promotes Glioblastoma Malignancy by sponging miR-7-5p. Cells. 2023; 12(6).
12. Chen H, Zhang P, Yu B, Liu J. The circular RNA circXPO1 promotes Tumor Growth via sponging MicroRNA-23a in prostate carcinoma. Front Oncol. 2021; 11712145.
13. Huang J, Shao Y, Gu W. Function and clinical significance of N6-methyladenosine in digestive system tumours. Exp Hematol Oncol. 2021;10(1):40.
14. Zheng G, Dahl JA, Niu Y, Fedorcsak P, Huang CM, Li CJ, et al. ALKBH5 is a mammalian RNA demethylase that impacts RNA metabolism and mouse fertility. Mol Cell. 2013;49(1):18–29.
15. Zhang Z, Wang L, Zhao L, Wang Q, Yang C, Zhang M, et al. N6-methyladenosine demethylase ALKBH5 suppresses colorectal cancer progression potentially by decreasing PHF20 mRNA methylation. Clin Transl Med. 2022;12(8):e940.
16. Yang D, Zhao G, Zhang HM. M(6)a reader proteins: the executive factors in modulating viral replication and host immune response. Front Cell Infect Microbiol 2023; 131151069.
17. Duan M, Liu H, Xu S, Yang Z, Zhang F, Wang G, et al. IGF2BPs as novel m(6)a readers: diverse roles in regulating cancer cell biological functions, hypoxia adaptation, metabolism, and immunosuppressive tumor microenvironment. Genes Dis. 2024;11(2):890–920.
18. Ma Y, Yang Y, Wang F, Wei Q, Qin H. Hippo-YAP signaling pathway: a new paradigm for cancer therapy. Int J Cancer. 2015;137(10):2275–86.
19. Shen H, Huang C, Wu J, Li J, Hu T, Wang Z et al. SCRIB promotes proliferation and metastasis by Targeting Hippo/YAP signalling in Colorectal Cancer. Front Cell Dev Biol 2021; 9656359.
20. Zhang Y, Yan S, Chen J, Gan C, Chen D, Li Y, et al. WWC2 is an independent prognostic factor and prevents invasion via Hippo signalling in hepatocellular carcinoma. J Cell Mol Med. 2017;21(12):3718–29.
21. Wang W, Wu L, Tian J, Yan W, Qi C, Liu W et al. Cervical Cancer cells-derived Extracellular vesicles containing microRNA-146a-5p affect actin dynamics to promote cervical Cancer metastasis by activating the Hippo-YAP Signaling Pathway via WWC2. J Oncol. 2022; 20224499876.
22. Yuan B, Yang J, Gu H, Ma C. Down-regulation of LINC00460 represses metastasis of Colorectal Cancer via WWC2. Dig Dis Sci. 2020;65(2):442–56.
23. Qiu S, Li B, Xia Y, Xuan Z, Li Z, Xie L, et al. CircTHBS1 drives gastric cancer progression by increasing INHBA mRNA expression and stability in a ceRNA- and RBP-dependent manner. Cell Death Dis. 2022;13(3):266.
24. Huang Q, Guo H, Wang S, Ma Y, Chen H, Li H, et al. A novel circular RNA, circXPO1, promotes lung adenocarcinoma progression by interacting with IGF2BP1. Cell Death Dis. 2020;11(12):1031.
25. Li J, Xu X, Xu K, Zhou X, Wu K, Yao Y, et al. N6-methyladenosine-modified circSLCO1B3 promotes intrahepatic cholangiocarcinoma progression via regulating HOXC8 and PD-L1. J Exp Clin Cancer Res. 2024;43(1):119.
26. Chen S, Zhang L, Su Y, Zhang X. Screening potential biomarkers for colorectal cancer based on circular RNA chips. Oncol Rep. 2018;39(6):2499–512.
27. Jiang Y, Hou J, Zhang X, Xu G, Wang Y, Shen L et al. Circ-XPO1 upregulates XPO1 expression by sponging multiple miRNAs to facilitate osteosarcoma cell progression. Exp Mol Pathol. 2020; 117104553.
28. Zhang L, Hou C, Chen C, Guo Y, Yuan W, Yin D, et al. The role of N(6)-methyladenosine (m(6)A) modification in the regulation of circRNAs. Mol Cancer. 2020;19(1):105.
29. Wu S, Yun J, Tang W, Familiari G, Relucenti M, Wu J, et al. Therapeutic m(6) a Eraser ALKBH5 mRNA-Loaded exosome-liposome hybrid nanoparticles inhibit progression of Colorectal Cancer in Preclinical Tumor models. ACS Nano. 2023;17(12):11838–54.
30. Ramesh-Kumar D, Guil S. The IGF2BP family of RNA binding proteins links epitranscriptomics to cancer. Semin Cancer Biol. 2022;86(Pt 3):18–31.
31. Ye M, Chen J, Lu F, Zhao M, Wu S, Hu C, et al. Down-regulated FTO and ALKBH5 co-operatively activates FOXO signaling through m6A methylation modification in HK2 mRNA mediated by IGF2BP2 to enhance glycolysis in colorectal cancer. Cell Biosci. 2023;13(1):148.
32. Wang J, Zhu M, Zhu J, Li J, Zhu X, Wang K, et al. HES1 promotes aerobic glycolysis and cancer progression of colorectal cancer via IGF2BP2-mediated GLUT1 m6A modification. Cell Death Discov. 2023;9(1):411.
33. Yang B, Wang YW, Zhang K. Interactions between circRNA and protein in breast cancer. Gene 2023; 895148019.
34. Ikeda Y, Morikawa S, Nakashima M, Yoshikawa S, Taniguchi K, Sawamura H et al. CircRNAs and RNA-Binding proteins involved in the Pathogenesis of cancers or Central Nervous System disorders. Noncoding RNA 2023; 9(2).
35. Fujita R, Zismanov V, Jacob JM, Jamet S, Asiev K, Crist C. Fragile X mental retardation protein regulates skeletal muscle stem cell activity by regulating the stability of Myf5 mRNA. Skelet Muscle. 2017;7(1):18.
36. Shang Q, Du H, Wu X, Guo Q, Zhang F, Gong Z, et al. FMRP ligand circZNF609 destabilizes RAC1 mRNA to reduce metastasis in acral melanoma and cutaneous melanoma. J Exp Clin Cancer Res. 2022;41(1):170.

Publisher's note